



# Influence of carbonate reservoir mineral heterogeneities on contact angle measurements

Jean Vicente Ferrari<sup>a,b,\*</sup>, Bruno Marco de Oliveira Silveira<sup>a</sup>, Jhonatan Jair Arismendi-Florez<sup>b</sup>,  
Thais Bortotti Fagundes<sup>b</sup>, Mayara Antunes da Trindade Silva<sup>a</sup>, Rodrigo Skinner<sup>c</sup>,  
Carina Ulsen<sup>a,b</sup>, Cleyton de Carvalho Carneiro<sup>a</sup>

<sup>a</sup> Universidade de São Paulo - Escola Politécnica, Integrated Technology for Rock and Fluid Analysis, Santos, SP, Brazil

<sup>b</sup> Universidade de São Paulo - Escola Politécnica, Laboratório de Caracterização Tecnológica, São Paulo, SP, Brazil

<sup>c</sup> Petrobras S.A. - Centro de Pesquisas Leopoldo Américo Miguez de Mello, Rio de Janeiro, RJ, Brazil

## ARTICLE INFO

### Keywords:

Carbonate  
SEM-MLA mineralogy  
Contact angle  
Wettability  
Pre-sal reservoir

## ABSTRACT

The wettability of reservoir rocks is one of the critical, advanced petrophysical parameters affecting oil production, during the field production life, from primary to enhanced recovery projects. This paper addresses the effect of mineral heterogeneities on wettability behaviour by measuring the contact angle (CA) on carbonate rock core samples from a Brazilian pre-salt reservoir. Mineralogical composition and mineral maps of samples extracted from reservoir plugs were characterised by X-ray based image analysis (scanning electron microscope coupled with automated mineral liberation analysis - SEM-MLA). The results indicated that around 99% of the samples were composed of calcite, dolomite, and quartz with completely different mineral distribution and texture. Also, the attained mineral maps directed the obtention of samples containing different mineral contents in which CA measurements were carried out by using the sessile drop method. CA experiments were run at a temperature of 60 °C and a pressure of 4000 psi with no-aged and aged samples in dead oil. Self-organised maps, generated by machine learning, were used to analyse the relationships between the variables. The results indicate that the predominant mineral constituents and their distribution influence the contact angle values and emphasise the importance of using reservoir core samples and their closest analogues when approaching rock/fluid interaction studies. Despite the samples with higher quartz content showing a greater water-phase affinity than carbonate ones, when both phases are inter-grown, wettability was changed to neutral and oil-wet. In this way, the mineral proportions and texture play a key role in the measured CA. Dolomite contributes to increasing the oil-wet tendency of the rock samples. Mineral maps are not currently applied in wettability studies but demonstrate that it can be a valuable tool for more reproducible measurements and a better understanding of the reservoir.

## Credit author contribution statement

Jean Vicente Ferrari: Conceptualization, Methodology, Writing – original draft, Writing – review & editing, Supervision. Bruno Marco de Oliveira Silveira: Conceptualization, Methodology, Investigation, Validation, Writing – original draft, Writing – review & editing. Jhonatan Jair Arismendi-Florez: Investigation, Writing – review & editing. Thais Bortotti Fagundes: Investigation, Validation, Writing – review & editing. Mayara Antunes da Trindade Silva: Investigation, Validation, Writing – review & editing. Rodrigo Skinner: Project administration, Resources. Carina Ulsen: Project administration, Funding acquisition,

Methodology, Writing – review & editing. Cleyton de Carvalho Carneiro: Project administration, Funding acquisition, Formal analysis, Writing – review & editing.

## 1. Introduction

Reservoir rocks are complex structures, in terms of their petrophysical and lithological features, which are generally heterogeneous. The permo-porosity heterogeneities of reservoirs, particularly those of the Brazilian pre-salt reservoirs (Rocha et al., 2019), in addition to the reservoir minerals' heterogeneity (Morrow, 1990; Najafi-Marghmaleki

\* Corresponding author. Universidade de São Paulo - Escola Politécnica, Integrated Technology for Rock and Fluid Analysis – Santos, SP, Brazil.  
E-mail address: [jeanferrari@usp.br](mailto:jeanferrari@usp.br) (J.V. Ferrari).

<https://doi.org/10.1016/j.petrol.2020.108313>

Received 15 October 2020; Received in revised form 14 December 2020; Accepted 24 December 2020  
Available online 29 December 2020  
0920-4105/© 2020 Elsevier B.V. All rights reserved.

et al., 2016) pose challenges for determining oil recovery strategies. Therefore, such heterogeneities link the rock properties and their interaction with fluids.

Generally speaking, reservoir minerals mainly comprise quartz, carbonate, and dolomite, each one having a different wettability, making the wetting of the composite rock difficult to describe (Abdallah et al., 2007). Moreover, the wettability may also be influenced by the water salinity, surface roughness, surface cleaning method, and oil aging conditions (Arif et al., 2020). Typically, the reservoir minerals are water-wet before oil migration (Abdallah et al., 2007).

Adsorption of organic surface-active compounds from crude oil (Ivanova et al., 2019) plays a critical role in determining the wetting properties of reservoir-rock surfaces (Al-Balushi et al., 2020; Morrow, 1990). Some of these polar compounds are acidic, such as carboxylic and naphthenic acids, being characterised by the total oil acid number (AN) (Al-Balushi et al., 2020). AN seems to be a key-parameter on the wetting nature of the reservoir (Zhang and Austad, 2005).

Overall, there is a consensus in the literature that most carbonate reservoirs have mixed or oil-wet wetting properties (Alotaibi et al., 2011; Ivanova et al., 2019). Rücker et al. (2019) reported that variation in surface charges, associated with the mineral composition, causes a variation of the local wettability. Mahani et al. (2015) stressed that most studies relate the charge at the carbonate rock/brine interface to the mineralogy of the rock, as well as the salinity, composition and, pH of the brine.

Carbonate rock tends to have a positively charged surface under common formation pH values (Deng et al., 2020). Rahimi et al. (2020) mention that such a positive charge favours the adsorption of negatively charged carboxyl groups in the crude oil, altering the carbonate surface, to become oil-wet. The surface charge appears to be critical to the oil adhesion and wettability alteration that leads to improved recovery from carbonates; electrostatic adhesive forces are the dominant control over carbonate reservoir wettability (Brady and Thyne, 2016).

Therefore, many studies have performed Zeta potential measurements to characterise surface charges that exit at the rock and mineral surfaces (Al-Balushi et al., 2020; Mahani et al., 2015). Shehata and Nasr-El-Din (2015) report values of Zeta potential measurements for sandstone, calcite and dolomite rock samples in seawater and 20%-diluted seawater at near-pH neutral conditions: the carbonate samples presented more positive values in comparison with the sandstone.

Because of the previously mentioned mechanisms, in wettability studies, the rock samples need to be restored to the original wettability of the reservoir by carrying out proper cleaning, drying and preparing for initial water saturation, followed by an oil-aging procedure (Ruidiaz et al., 2018). In this way, effects related to surface mineral chemistry, oil and aqueous phase composition, contact time, temperature and pressure may be taken into account (Al-Balushi et al., 2020; Alotaibi et al., 2011; Arif et al., 2020).

Amirpour et al. (2015) emphasised that wettability is, perhaps, the most critical factor affecting the rate of oil recovery and the residual oil saturation, which is the target of enhanced oil recovery strategies. The most widely used wettability measurement techniques include contact angle measurement, Amott test, Amott–Harvey Test and United States Bureau of Mines (USBM) (Deng et al., 2020).

The contact angle is a universal measure of the wettability of surfaces (Morrow, 1990) and is being used to characterise whether something is water-wet (low oil adhesion) or oil-wet (high oil adhesion) (Brady and Thyne, 2016). Rücker et al. (2019) mentioned that natural rocks containing crude oil are often mixed-wet, in which the wettability varies across the pore space due to changing local contact angle values.

Static contact angle measurements can be carried out in slices from analogous outcrop rock (Kanj et al., 2020) and reservoir rock samples (Najafi-Marghmaleki et al., 2016). Alternatively, pure minerals can also be used (Al-Balushi et al., 2020; Drexler et al., 2019). Anderson (1986b) stressed that a reservoir rock contains many different constituents,

causing localised heterogeneous wettability influencing the contact angle measurements. In this way, there is an obvious limitation when using a relatively pure mineral to represent reservoir rocks in such measurements (Anderson, 1986b; Morrow, 1990). Moreover, because the mineral constituents play a critical role in these measurements, there are also disadvantages when using outcrop rock samples. In this respect, Najafi-Marghmaleki et al. (2016) reported that one of the advantages of performing contact angle measurements on large surfaces is that multiple droplets can be deposited in various locations on the sample to determine heterogeneities.

Arif et al. (2020) mentioned that despite what has been published elsewhere, there is significant uncertainty associated with the current carbonate wettability data. In their work, four carbonate reservoir rock core samples, with mineralogy ranging from 100% calcite to 100% dolomite, were characterised by X-Ray Diffraction (XRD) analysis and used to investigate the carbonate wettability as a function of mineral constituents in reservoir brine medium. The authors reported different hydrophilicity for the samples due to their mineral composition, with the pure calcite samples being more hydrophilic in comparison to the dolomite. They emphasised that using calcite as an analogous mineral for carbonate rock is not entirely justified for contact angle measurements.

Because the reservoir rock mineralogy is also a key-parameter in studies on wettability properties, mineralogical core sample analysis must be carried out, using the scanning electron microscope (SEM) or mineral liberation imaging analysis (MLA) (SEM-MLA) (Minde et al., 2020). SEM-MLA analysis has also been used to characterise the wettability of oil-aged samples (at low vacuum conditions) (Sripal and James, 2018).

This work aims to correlate the main mineral groups (characterised by the SEM-MLA technique on carbonate rock core samples) from a Brazilian pre-salt reservoir by using contact angle measurements, with a focus on addressing the influence of mineral heterogeneity on the wettability tendency in a reservoir.

## 2. Materials and methods

In this section, all analytical procedures that were performed to evaluate and understand the wettability heterogeneity considering the mineralogical influence will be described in detail.

### 2.1. Mineralogical characterisation – SEM/MLA

Mineralogical characterisation of the samples was carried out with the aim of identifying the areas to be later analysed by CA. The sub-sample selection procedure is summarised in Fig. 1. For this study, eight different carbonate plugs were characterised.

Initially, images from the plugs (Fig. 1-a) were obtained by 3D microtomography (X ray microscope at Xradia/Zeiss Versa XRM-510) to identify areas containing fractures or vugs, avoiding cutting slices in these regions (Fig. 1-b). The plug dimensions were approximately 6.0 cm high and 3.8 cm diameter (1.5 inches). The image acquisition conditions were set at: voltage of 160 kV, power of 10 W, number of acquisitions 1,000, time per acquisition of 4.7 s, detector resolution of 1024 x 1024 px and the attained pixel size was approximately 40–50  $\mu$ m.

Radial slices (approximately 0.5 cm high) were obtained from the top or bottom of the plugs by using a metallographic cutter (Fig. 1-c), followed by drying in an oven at 40 °C.

From the radial slices obtained from the plugs (Fig. 1-d), another fragment was extracted (Fig. 1-e) perpendicular to the grain orientation to enhance the representativeness of the mineral composition. Its dimensions were approximately 1.0 cm width, 0.5 cm height and 3.0 cm (1.5") length (plug diameter), and it was divided into two (Fig. 1-f,g) for a better quality of sample preparation and polishing procedure.

The samples were embedded (Fig. 1-h) with epoxy resin (Struers brand) in a cylindrical mould of 30 mm diameter (Fig. 1-h) and then

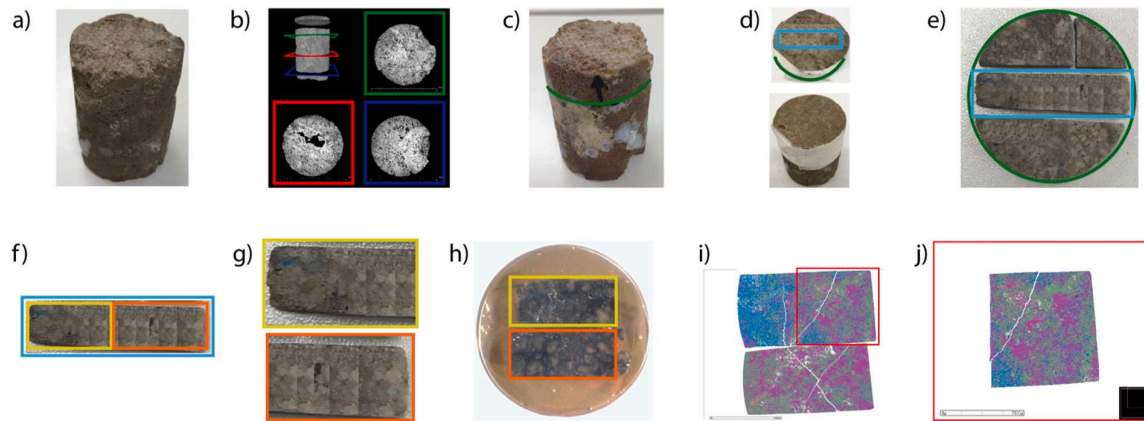


**Fig. 1.** General scheme of plug mineralogical characterisation. a. Original plug sample; b. Image from microtomography (example of three slices); c. Slice selection; d. Slice cutting and axial cut perpendicular to the grain orientation; e and f. Selecting and cutting the central slice area; g. Fragments for SEM/MLA analysis; h. Polished section containing the two fragments; i. Mineral mapping; j. Selected area for contact angle measurements.

placed in a vacuum (0.03 Pa) for 12 min in the CITOVAC equipment (Struers brand) to remove bubbles. After that, the sections were stored at room temperature to cure the resin for 24 h. After hardening, the samples were removed from the supports for the grinding and polishing process (Tegramim 40 machine - Struers brand), starting with 220 sandpaper and ending with a diamond solution of 1  $\mu\text{m}$ . This polishing procedure was performed to reduce the roughness effect on CA measurements (Prydatko et al., 2018). After polishing, the samples were immersed in water and cleaned in an ultrasound bath for 3 min and then dried in an oven at 45  $^{\circ}\text{C}$ . After drying, the polished sections were covered with carbon (approximately 10 nm) through the evaporation method, by carbon wire evaporator (BAL-TEC model SCD 050) and analysed by MEV-MLA (Fig. 1-i,j).

The detailed mineralogical study of the forms of occurrence and mineral association was carried out by semi-automated image analysis using MLA software (Mineral Liberation Analyser – FEI) coupled to SEM (Quanta 650 FEG - FEI) with an energy dispersion spectrometer (EDS) (Espirit - Bruker).

The SEM operating conditions were set to guarantee the resolution for the textural features found (pixel size of 2.21  $\mu\text{m}$ ) and brightness, contrast and scanning speed (16  $\mu\text{s}$ ) were adjusted to allow adequate discrimination between shades of grey in the backscattered electrons images (BSE). The image analysis was carried out in XBSE mode, that analyses each phase (areas of consistent BSE grey value) with a single centroid X-ray point. GXMAP mode was used for distinguishing quartz and dolomite due to the similarity of grey levels (similar atomic weight between the minerals), which performs X-ray mapping in the triggered phases. The parameters set for the SEM/MLA analysis are shown in Table 1.

The mineral maps from MLA guided further area selection and cuts (Fig. 1-i) in order to obtain two pieces of rock fragments that contained areas predominant in each mineral and a mixture of these components (Fig. 1-j).

Carbon coating was removed by isopropyl alcohol solution and placed in an ultrasound bath for 5 min. Further cuts were carried out based on the dimension requirements needed to arrange them on the slice holder inside the (high pressure and high temperature) HPHT cell, as will be presented.

## 2.2. Contact angle (CA) measurements

### 2.2.1. Test protocol

The experimental test protocol is presented in Fig. 2. The flowchart represents each step performed to characterise the surface of the carbonate rock samples, identifying mineralogical content and its

**Table 1**

Parameters for SEM/MLA analysis.

Parameter	Details
Section diameter ( $\mu\text{m}$ )	30000
Mode	XBSE/GXMAP
Acceleration (kV)	20
Spot	5.80
Aperture ( $\mu\text{m}$ )	40.00
Working distance (mm)	14
Contrast	26.5
Brightness	78
Counts kcps at quartz	520.0
<b>Grey level</b>	
Magnesite	50
Quartz/dolomite	78
Calcite	100
Pyrite	220
<b>Image</b>	
Scan speed: ( $\mu\text{s}$ )	16
Magnification	250X
Resolution: (px)	500
Pixel size ( $\mu\text{m}$ )	2.21
<b>X-ray Mapping (GXMAP)</b>	
X-ray trigger	Quartz-dolomite
Step size (px)	6
Start channel	38
<b>Average (image acquisition time (per sample/section)</b>	2 h

wettability by contact angle (CA) measurements at HPHT conditions.

The experiments were carried out using dead oil, synthetic formation water (SFW) and rock samples from a Brazilian pre-salt carbonate reservoir.

### 2.2.2. Fluids for CA measurements

The SFW is a high salinity and hardness brine used as the external phase in CA measurements. The ionic composition, based on the target reservoir formation water, is presented in Table 2.

The droplet was a dead oil phase with the following features: 29.5 $^{\circ}$ API, acid number of 0.57 mg KOH/g and density and viscosity (60  $^{\circ}\text{C}$  and 4000 psi) of 0.8884 g/cm $^3$  and 25.03 mPa.s, respectively. Additionally, the oil-SFW interfacial tension value (IFT) under test conditions was 9.66 mN/m.

### 2.2.3. Cleaning, saturation, and SFW aging process

The samples selected for CA analyses were slightly cleaned. Toluene was applied, using soft paper, to remove organic compounds and then the rock surface was allowed to dry naturally. Methanol was applied to remove inorganic compounds.



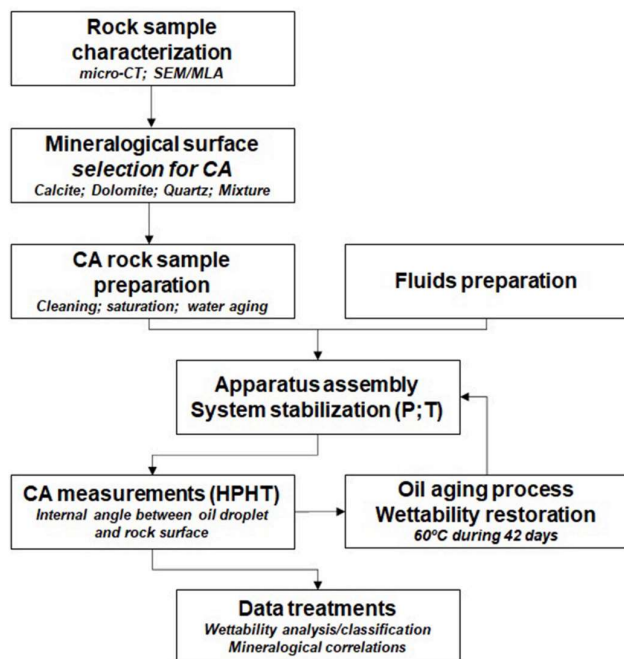


Fig. 2. Test protocol for mineralogical characterisation and CA measurements.

Table 2  
Synthetic formation water composition and properties.

Ion	Na <sup>+</sup>	K <sup>+</sup>	Mg <sup>2+</sup>	Ca <sup>2+</sup>	Cl <sup>-</sup>	SO <sub>4</sub> <sup>2-</sup>	HCO <sub>3</sub> <sup>-</sup>
mg/L	68,980	3,458	1,674	7,410	127,467	39	18

SFW solution: pH = 7.7 and density = 1.14 g/cm<sup>3</sup>

After that, the cleaned and dried rock samples were then immersed in glass reagent bottles containing the SFW for the saturation process, carried out under vacuum conditions at room temperature. The bottles were then closed and placed into an air-bath at 60 °C for the 24 h SFW aging process, followed by cooling at room temperature and initial CA measurements.

According to the literature, the water aging procedure is recommended to be performed before the oil aging procedure (Gupta and Mohanty, 2008; Hamouda and Gomari, 2006; Sharma and Mohanty, 2013).

#### 2.2.4. Oil aging

The oil aging process was performed after the first measurements, when the samples had only been SFW aged. For this, the rock samples were cleaned with soft paper, immersed in SFW, dried with absorbent paper, and then immersed in dead oil glass reagent bottles. After these procedures, the bottles were placed into an air-bath at 60 °C for up to 42 days. This represented the oil aging process.

In this way, it was possible to verify whether the aging time would influence the wettability of the sample, by comparing the CA values of the same surface in two distinct periods: before and after 42 days of oil aging. The best practice for oil aging is still unclear, with various studies adopting aging times from 1 to 60 days (Branco and Gil, 2017; Chen et al., 2018; Gupta and Mohanty, 2008; Hamouda and Gomari, 2006; Sharma and Mohanty, 2013).

#### 2.2.5. Apparatus assembly and measurements

The system used was an HPHT apparatus for interfacial tension, surface tension and contact angle measurements: a model IFT Cell Part No 10, from Core Lab Instruments. The system allows measurements

over a wide range of temperatures and pressures, up to 200 °C and 10,000 psi, respectively. The accuracy and precision of the measurement system is  $\pm 0.1^\circ$  and  $0.01^\circ$ , respectively. Fig. 3 shows the detailed schematic diagram of the whole apparatus.

For the CA measurements, the rock samples should be fixed in the sample holder. For this, it is necessary to remove the excess of adhered oil in the rock sample during the oil aging process. However, there is no consensus on the procedures and solvents that should be applied for this purpose (Ahmadi et al., 2020; Fani et al., 2018; Teklu et al., 2015).

Thus, the removal process without the application of organic solvent was adopted. Firstly, the oil was carefully removed from each rock sample with absorbent paper, until no more oil transferred from the rock to the paper, followed by immersion in SFW and then, dried with soft paper. The rock was then attached to the sample holder with double-sided tape and placed into the HPHT cell, as can be observed in Fig. 4.

After the apparatus was assembled, the external fluid was manually pumped into the HPHT cell, followed by the dead oil droplet on the rock surface. As the oil droplet was injected manually, to avoid the droplet size effect reported in the literature (Drelich et al., 1996; Drelich, 1997; Prydatko et al., 2018), all experiments were performed with smooth surfaces and the oil droplet injection was performed using same needle (0.793 mm ID and 1 mm OD). To set up the experimental conditions, the desired pressure was imposed by SFW injection and the backpressure valve adjusted. The temperature was adjusted by a digitally-controlled heating blanket. The pressure setting was 4000 psi, and the temperature was 60 °C. This temperature is associated with the maximum value of further wettability experiments with reservoir cores in ultra-centrifuge systems, such as USBM and Amott measurements (not addressed here).

To analyse the internal angle between the droplet and rock surface, the captive bubble method was applied. The DROPImage software was used, and online monitoring of the right and left angles was carried out simultaneously or individually. The choice was based on the parity of the baseline to the flat shape of the sample surface, as shown in Fig. 5.

The adopted criteria for classifying rock wettability was: oil wettability tendency - CA ranging from 0° up to 75°, intermediate/neutral - CA from 75° up to 105° and or water wettability - CA from 105° up to 180° (Anderson, 1986; Anderson, 1986b).

The experimental data was recorded after the entire system reached equilibrium, i.e. pressure, temperature, and CA value. The time required for this purpose was about 60 min. The reported final values of CA were the average of at least ten points. All points were measured every 60 s, until the end of the experiment.

The final procedure performed was the apparatus clean-up. To avoid any contamination and possible interference in the other runs, at the end of each experiment, the organic and inorganic phases were removed for the next run. The whole system was cleaned by flushing with kerosene, isopropyl alcohol, and distilled water. After that, the lines were dried with dry air, and the other components with absorbent soft paper.

#### 2.3. Integrated visualisation of variables using self-organising maps (SOM)

Data were also analysed by using a machine learning technique called SOM (Haykin, 2008; Kohonen, 1995) to observe the relationships between the variables in a synthetic and integrative way. SOM technique is a kind of artificial neural network with unsupervised learning and consists of treating the samples as vectors in an n-dimensional space, defined by a set of variables. The n-dimensional space will later be projected on a self-organised map with previously defined dimensions and a number of neurons. After competitive and collaborative steps, each original sample is represented by a best-matched unity (BMU). These BMUs are projected on maps preserving the topological relationships of similarity between the samples, measured by the Euclidean distance, aggregating the nonlinear relationships of the set of variables.



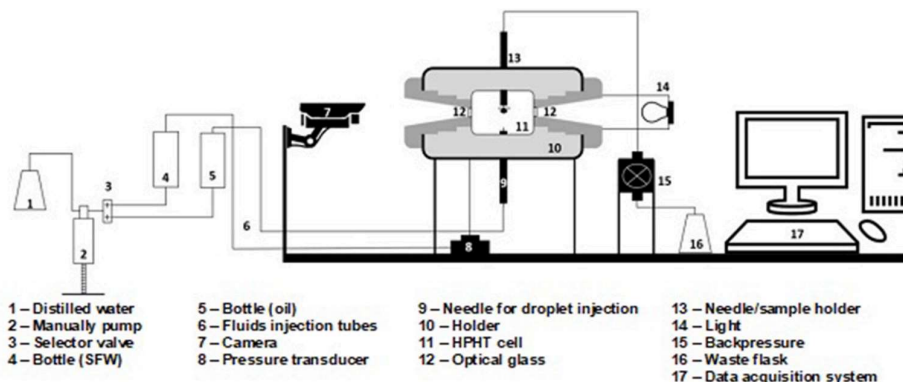


Fig. 3. Schematic diagram of CA experimental apparatus.

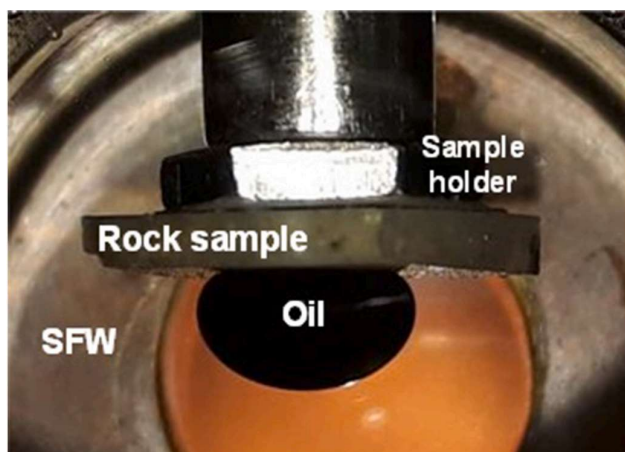


Fig. 4. Picture of the system SFW/oil/rock sample inside the HPHT cell.

For each sample analysed, the results of the mineralogical compositions, oil aging, contact angle and wettability were inserted as vectors. A map with dimensions of 20 x 20 cells (totalling 400 neurons) was used to generate the projection on a toroidal hypersurface. The number of neurons being higher than the number of samples was purposeful, because of the demand for visualisation and, therefore, the formation of well-defined regions among BMU's. Finally, component plots (CP) and unified distance matrix (U-Matrix) maps were produced, where the samples after the oil aging process were marked by an asterisk (\*). The results of these construction processes can be seen on the maps presented in Fig. 9.

### 3. Results and discussion

The mineralogical distribution and its classification on the rock sample surfaces by the SEM/MLA is presented in Fig. 6. From the eight characterised samples, four were chosen to represent this procedure.

Examples from mineral mapping of four fragments: (a) C1 - calcite, (b) D1 - dolomite, (c) Q1 - quartz, (d) M1 - mixture; the highlighted squares exemplify the selected areas for CA measurements. Scale bars shown in the lower-left corner of figures – 1 cm.

According to the SEM/MLA results, the samples presented similar mineralogical compositions but very heterogeneous mineral distribution and texture, as clearly shown by the images in Fig. 6. The main minerals identified in all samples were calcite (C), dolomite (D), and quartz (Q), in addition to the mixture (M) of all three (inter-grown in different proportions and texture). In each image, there is a highlighted square area that exemplifies some of the mineral distributions. For example, the images refer to the 1 cm wide sample surface, extracted from the radial slices. Fig. 6-c shows that the preponderant mineral constituent at the centre is quartz, with calcite constituents next to the borders and inter-grown with dolomite.

The sample areas C1(a), D1(b), Q1 (c) and M1 (d) presented in Fig. 6, in addition to areas C2, D2, Q2 and M2 (images not shown here), were used to run the CA experiments and to evaluate the mineralogical influence on reservoir rock wettability. Table 3 presents the identification of the sample considering the main mineral content, the mineralogical composition (phase proportion) of each sample (fragment 1 and 2) and CA values under 60 °C and 4000 psi, before and after 42 days of the oil aging process.

Calcite, dolomite, and quartz represented more than 99% of the mineral content in all samples. The exception was the sample D2, with 96.76% of the mentioned minerals and 2.67% of magnesite. Moreover, the samples presented less than 1% of other minerals, such as fluorite, barite, pyrite, monazite, K-feldspar, muscovite, Al–Na–O, F–Na–Al–Si, Apatite, Al–P–Sr–Ba and Si–Ti.

About the wettability classification of the samples tested, Fig. 7

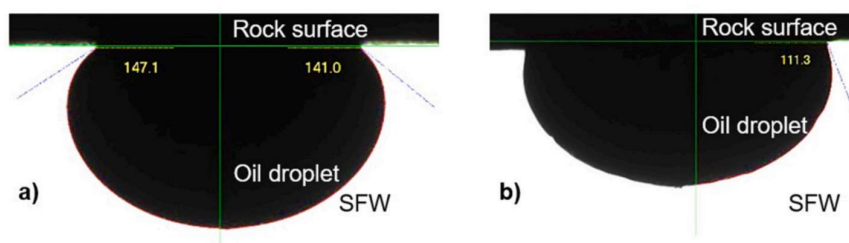


Fig. 5. Pictures of the droplets showing the baseline and the contact angles of SFW/oil/rock by captive bubble method. a) Simultaneous measurements. b) Individual measurement.

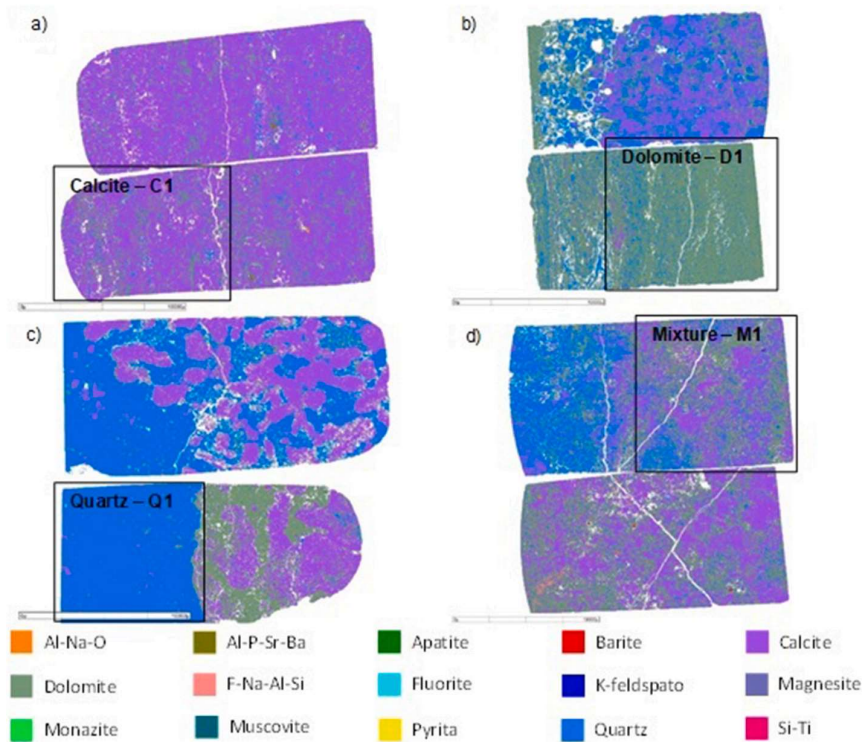


Fig. 6. Mineral distribution and classification on rock surfaces by SEM/MLA.

**Table 3**  
Samples identification, mineralogical composition and CA values.

Predominant mineral		Calcite		Dolomite		Quartz		Mixture	
Sample		C1	C2	D1	D2	Q1	Q2	M1	M2
Main mineral content	Quartz	3.76%	2.47%	12.83%	7.30%	93.93%	55.06%	16.27%	23.29%
	Dolomite	25.59%	16.05%	85.42%	89.37%	3.47%	25.86%	45.40%	49.99%
	Calcite	69.93%	81.23%	1.52%	0.09%	2.52%	18.67%	37.96%	25.85%
CA values	No oil aging	78.96	110.26	89.59	73.60	144.04	106.34	131.52	107.90
	Oil aged	32.88	62.57	55.66	36.07	124.34	66.82	33.39	82.03

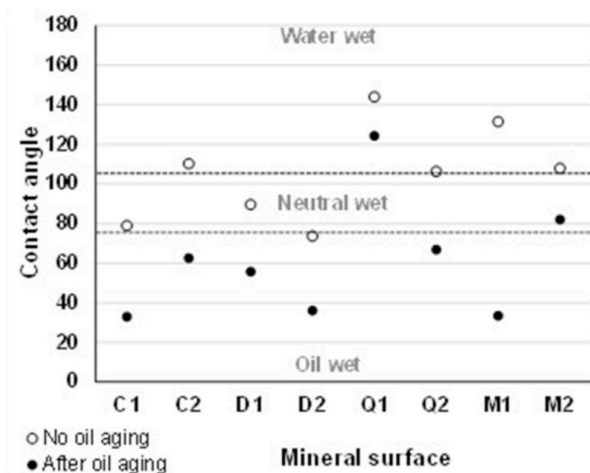


Fig. 7. Contact angle among SFW/oil/rock surface under 60 °C and 4000 psi.

summarises the data considering the measurements of internal angles.

According to the presented data, it is possible to observe the oil aging influence in the CA values and, consequently, in the wettability tendency. Before the oil aging process, the higher values of contact angles were observed in each rock sample, concentrating in neutral and water wet regions (angles  $> 75^\circ$ ). The highest degree of hydrophilia is associated with the rock samples' clean-up procedures. The solvents applied to remove organic and inorganic compounds from the rock surface changes the original wettability tendency to water-wet (Anderson, 1986; Marzouk, 1999; Okasha et al., 2007). After oil aging, the hydrophobic degree of SFW increased for all samples, indicated by the CA values in the oil-wet region (angles  $< 75^\circ$ ), except Q1 and M2. For these samples, the CA values represented water and neutral-wet, respectively.

As already pointed-out, this behaviour may be due to the organic compounds' adsorption of the oil phase on rock surfaces during the aging process, restoring the original tendency of the rock samples' wettability (Chen et al., 2018; Drexler et al., 2019; Esfahani and Haghighi, 2004; Sharma and Mohanty, 2013).

The influence of the predominant mineral on the rock sample wettability was evaluated by the data presented in Table 3, Fig. 7 and, also, the reduced CA values presented in Fig. 8. In these data, no oil aging condition was considered as a benchmark.

For calcite, dolomite, and quartz samples, the CA reductions ranged

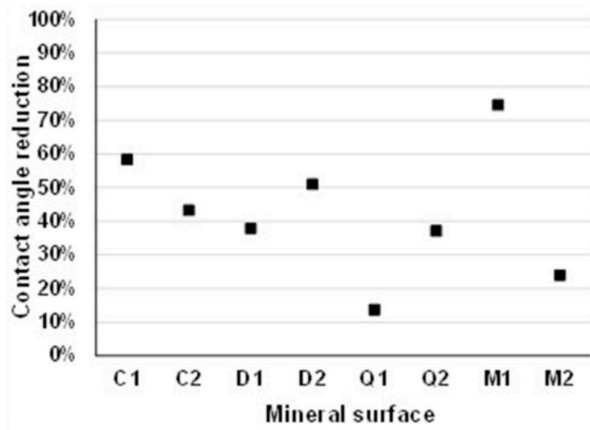


Fig. 8. Mineral influence on the aging process and CA reduction.

from 43% to 58%, 38%–51%, and 14%–37%, respectively. This indicates that carbonate minerals presented a higher affinity to the organic phase, contributing to the oil-wet tendency.

The opposite trend can be assigned to the quartz mineral. The higher its concentration in the rock surface, the lower was the CA reduction.

This can be seen by comparing the results between the Q1 and Q2 samples. With 93% of quartz content, the Q1 sample showed that the oil aging process did not change the sample wettability, i.e. the wet water tendency was maintained. However, in the Q2 sample, with 55% of quartz content and, consequently, higher concentrations of carbonate minerals, the wettability was changed from neutral to oil-wet after the aging process.

Furthermore, in Fig. 7 we observe higher CA values for the Q2 sample than for carbonate ones, such as C1, C2, D1, and D2. Also, the Q2 sample presented a lower CA reduction than C1, C2, D1, and D2, as shown in Fig. 8. These data indicate that quartz minerals can increase the hydrophilic degree of the rock surface. This can be confirmed by comparing the results within a fragment sample category, where those fragments with relatively higher concentrations of quartz (such as D1, Q1, and M2) presented the higher values of CA and lower CA reductions after oil aging.

Another effect observed by analysing the results within a fragment sample category, was that dolomite can contribute to increasing the oil-wet tendency of the rock samples. Fragments that showed relatively higher concentrations of dolomite (e.g. samples C1, D2, and Q2) presented lower values of CA and higher CA reductions after oil aging. The exception was for the mixed samples: although sample M2 presented a higher concentration of dolomite, it also showed higher quartz content than the M1 sample. Thus, for sample M2, the hydrophilic effect of

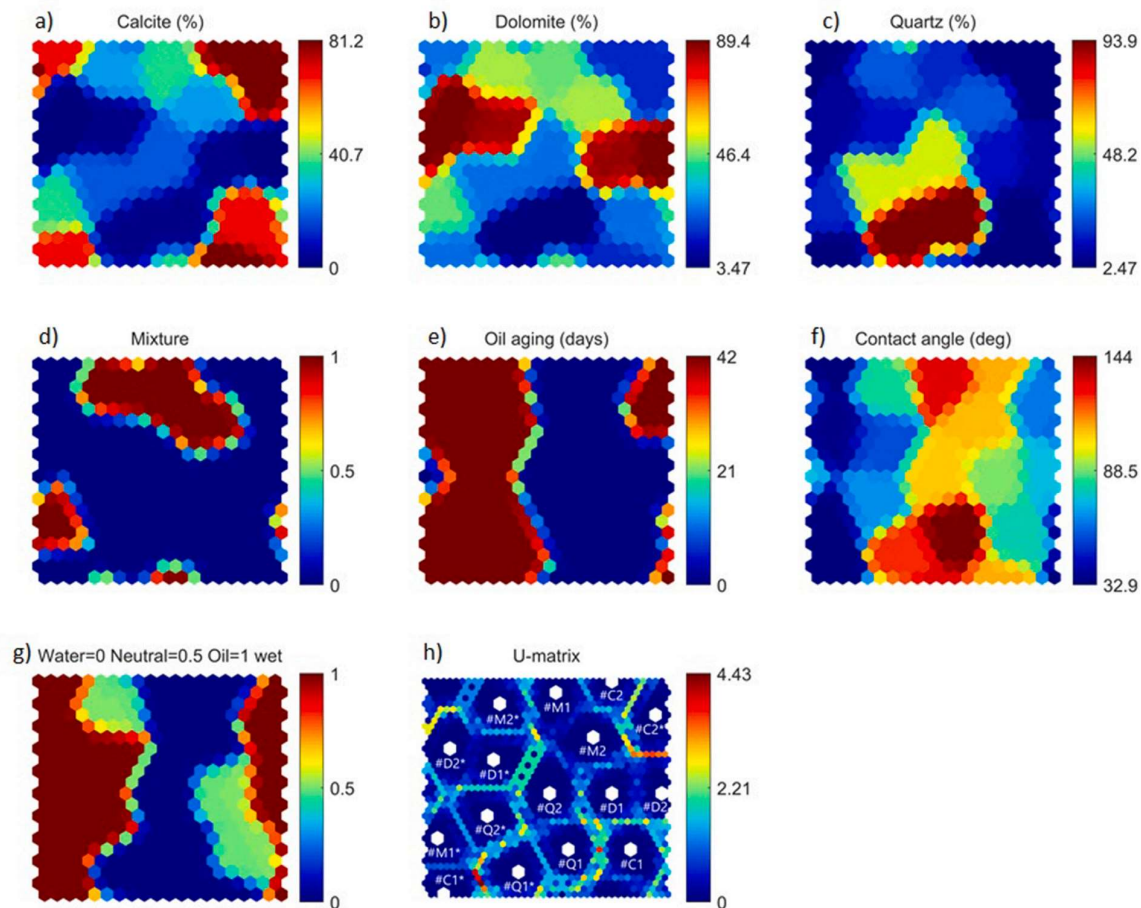


Fig. 9. Self-organised maps showing component plots and U-Matrix. a) concentration with a predominance of quartz; b) mineralogical composition with a predominance of dolomite; c) mineralogical composition with a predominance of calcite; d) mixed mineral proportions; e) aging in oil; f) contact angle; g) water, neutral or oil wettability; and h) U-Matrix, showing the samples grouped topologically based on similarity. In (H) the warm colours indicate higher dissimilarity and cold colours indicate greater similarity. Also, samples after the oil aging process were marked by an asterisk (\*).



quartz also contributed to the measured CA values. Hence, the mineralogical composition effects were also observed in the wettability of the mixed samples after the oil aging process. The M1 sample, with higher carbonate mineral contents, was classified as oil-wet, while M2, with higher quartz content, showed a neutral wettability.

From the integrated analysis developed by the SOM machine learning algorithm, it was possible to visualise the integral relationships between the variables on maps. Fig. 9 shows: (A to D) the percentage of minerals, as well as mixing zones; (E) regions of aging and non-aging in oil; (F) contact angle variations; (G) water-wettability (in blue), neutral-wettability (in green) and oil-wettability (in red); and (H) U-matrix with white hits related to the analysed samples. In the last map (H), colder colours represent more similar regions and warm colours represent borders of high dissimilarity between samples. Additionally, samples after the oil aging process were marked by an asterisk (\*).

According to the maps, oil aging was able to alter the wettability of the Q2 sample, which contains 55% quartz, from water-wet to oil-wet. However, for the Q1 sample, with ~94% quartz, water-wet was maintained after oil aging, despite the small decrease in the CA. Oil aging in sample D1 was responsible for decreasing the CA and changing the neutral-wet to oil-wet. It is worth mentioning that the sample D2, with 89.4% dolomite and 7.3% quartz, has less quartz than D1, characterised by 84% dolomite and 12% quartz. In sample D2, the oil-wet behaviour was maintained after oil aging. Samples dominated by calcite tended to alter wettability with oil aging. In C1, oil aging considerably decreased the CA, changing the wettability from neutral to oil-wet. Sample C2, which was initially water-wet, became oil-wet after oil aging.

Despite the samples with higher quartz content showing more water phase affinity than carbonate ones, when both phases are inter-grown, wettability was changed to neutral to oil-wet; the carbonate minerals presented a more oil-wet tendency than quartz. Moreover, the dolomite influence to increase the hydrophobic degree of the rock samples was similar to the data reported by Arif et al. (2020) for rock samples with 61% of calcite and 39% of dolomite in its constitution. Regarding quartz influence on the wettability, the data are consistent with its higher affinity to the aqueous phase, compared with the carbonate minerals (Wang and Gupta, 1995).

#### 4. Conclusions

The rock samples extracted from plugs of a Brazilian Pre-Salt carbonate reservoir presented high heterogeneity, in terms of mineralogical distribution and texture, despite the similar occurrence of minerals, which directly affects its wettability behaviour. The SEM/MLA results showed that calcite, dolomite, and quartz were the main minerals quantified in the samples analysed.

The mineralogical content influenced the contact angle values at 60 °C and 4000 psi. The highest hydrophobic degree was observed in carbonate minerals, mainly those with higher dolomite content. Quartz-dominated minerals tend to increase the sample surfaces hydrophilic degree.

Both calcite and dolomite samples presented an oil-wet tendency. The sample with 93% of quartz showed water-wet tendency, while the sample with 55% of quartz was classified as oil-wet.

The oil aging was a fundamental process for restoring the wettability of the sample after cleaning. For all samples, the contact of dead oil on mineral surfaces during aging, increased the hydrophobic degree.

This work provides important support to the wettability test result analysis and its findings can also be used as input data in reservoir simulation models and machine learning studies for predicting reservoir wettability. Besides, the precise characterisation of mineral distribution and associations can lead to a future determination of the proportion of each mineral that is exposed to the surface of the pores.

#### Declaration of competing interest

The authors declare that they have no known competing financial interests or personal relationships that could have appeared to influence the work reported in this paper.

#### Acknowledgements

The authors acknowledge the funding and support from Petrobras S. A./CENPES (Centro de Pesquisas e Desenvolvimento Leopoldo Américo Miguez de Mello), Brazil, Process number 2016/00126-2.

#### References

- Abdallah, W., Buckley, J.S., Carnegie, A., Edwards, J., Fordham, E., Graue, A., Herold, B., Habashy, T., Seleznev, N., Signer, C., Hussain, H., Montaron, B., Ziauddin, M., 2007. Fundamentals of wettability. *Oilfield Rev.* 19, 44–61. <https://www.slb.com/-/media/files/oilfield-review/p44-61-english>.
- Ahmadi, S., Hosseini, M., Tangestani, E., Mousavi, S.E., Niazi, M., 2020. Wettability alteration and oil recovery by spontaneous imbibition of smart water and surfactants into carbonates. *Petrol. Sci.* 17, 712–721. <https://doi.org/10.1007/s12182-019-00412-1>.
- Al-Balushi, M.A., Karimi, M., Al-Maamari, R.S., 2020. Impact of acid and base numbers and their ratios on wettability alteration of the calcite surface. *Energy Fuels* 34, 245–257. <https://doi.org/10.1021/acs.energyfuels.9b03538>.
- Alotaibi, M.B., Nasralla, R.A., Nasr-El-Din, H.A., 2011. Wettability studies using low-salinity water in sandstone reservoirs. *SPE Reservoir Eval. Eng.* 14, 713–725. <https://doi.org/10.2118/149942-PA>.
- Amirpour, M., Shadizadeh, S.R., Esfandiyari, H., Ahmadi, S., 2015. Experimental investigation of wettability alteration on residual oil saturation using nonionic surfactants: capillary pressure measurement. *Petroleum* 1, 289–299. <https://doi.org/10.1016/j.petm.2015.11.003>.
- Anderson, W., 1986. Wettability literature survey- Part 2: wettability measurement. *J. Petrol. Technol.* 38 <https://doi.org/10.2118/13933-PA>.
- Anderson, W.G., 1986. Wettability literature survey- Part 1: rock/oil/brine interactions and the effects of core handling on wettability. *J. Petrol. Technol.* 38, 1. <https://doi.org/10.2118/13932-PA>.
- Arif, M., Abu-Khamsin, S.A., Zhang, Y., Iglauer, S., 2020. Experimental investigation of carbonate wettability as a function of mineralogical and thermo-physical conditions. *Fuel* 264, 116846. <https://doi.org/10.1016/j.fuel.2019.116846>.
- Brady, P.V., Thynne, G., 2016. Functional wettability in carbonate reservoirs. *Energy Fuels* 30, 9217–9225. <https://doi.org/10.1021/acs.energyfuels.6b01895>.
- Branco, F.R., Gil, N.A., 2017. NMR study of carbonates wettability. *J. Petrol. Sci. Eng.* 157, 288–294. <https://doi.org/10.1016/j.petrol.2017.06.023>.
- Chen, Y., Xie, Q., Sari, A., Brady, P.V., Saeedi, A., 2018. Oil/water/rock wettability: influencing factors and implications for low salinity water flooding in carbonate reservoirs. *Fuel* 215, 171–177. <https://doi.org/10.1016/j.fuel.2017.10.031>.
- Deng, X., Kamal, M.S., Patil, S., Hussain, S.M.S., Zhou, X., 2020. A review on wettability alteration in carbonate rocks: wettability modifiers. *Energy Fuels* 34, 31–54. <https://doi.org/10.1021/acs.energyfuels.9b03409>.
- Drelich, J., 1997. The effect of drop (bubble) size on contact angle at solid surfaces. *J. Adhes.* 63, 31–51. <https://doi.org/10.1080/00218469708015212>.
- Drelich, J., Miller, J.D., Good, R.J., 1996. The effect of drop (bubble) size on advancing and receding contact angles for heterogeneous and rough solid surfaces as observed with sessile-drop and captive-bubble techniques. *J. Colloid Interface Sci.* 179, 37–50. <https://doi.org/10.1006/jcis.1996.0186>.
- Drexler, S., Souza, F.P., Correia, E.L., Silveira, T.M.G., Couto, P., 2019. Investigation OF the key parameters affecting wettability OF a BRAZILIAN pre-salt crude oil and brine ON pure minerals through statistical analysis. *Braz. J. Pet. Gas* 12, 195–204. <https://doi.org/10.5419/bjppg2018-0018>.
- Esfahani, M.R., Haghighi, M., 2004. Wettability evaluation of Iranian carbonate formations. *J. Petrol. Sci. Eng.* 42, 257–265. <https://doi.org/10.1016/j.petrol.2003.12.016>.
- Fani, M., Al-Hadrami, H., Pourafshary, P., Vakili-Nezhaad, G., Mosavat, N., 2018. Optimization of smart water flooding in carbonate reservoir. In: Abu Dhabi International Petroleum Exhibition & Conference. Presented at the Abu Dhabi International Petroleum Exhibition & Conference., Society of Petroleum Engineers, Abu Dhabi, UAE. <https://doi.org/10.2118/193014-MS>.
- Gupta, R., Mohanty, K.K., 2008. Wettability alteration of fractured carbonate reservoirs. In: SPE Symposium on Improved Oil Recovery. Presented at the SPE Symposium on Improved Oil Recovery. Society of Petroleum Engineers, Tulsa, Oklahoma, USA. <https://doi.org/10.2118/113407-MS>.
- Hamouda, A.A., Rezaei Gomari, K.A., 2006. Influence of temperature on wettability alteration of carbonate reservoirs. In: SPE/DOE Symposium on Improved Oil Recovery. Presented at the SPE/DOE Symposium on Improved Oil Recovery. Society of Petroleum Engineers, Tulsa, Oklahoma, USA. <https://doi.org/10.2118/99848-MS>.
- Haykin, S., 2008. *Neural Networks and Learning Machines*, 3<sup>rd</sup> ed. Prentice Hall, New York.
- Ivanova, A., Mitirev, N., Cheremisin, A., Orekhov, A., Kamysinsky, R., Vasiliev, A., 2019. Characterization of organic layer in oil carbonate reservoir rocks and its effect on microscale wetting properties. *Sci. Rep.* 9, 10667. <https://doi.org/10.1038/s41598-019-47139-y>.

- Kanj, M., Sakthivel, S., Giannelis, E., 2020. Wettability alteration in carbonate reservoirs by carbon nanofluids. *Colloids Surf. Physicochem. Eng. Asp.* 598, 124819. <https://doi.org/10.1016/j.colsurfa.2020.124819>.
- Kohonen, T., 1995. *Self-Organizing Maps*, 1<sup>st</sup> ed. Springer, Berlin ; New York.
- Mahani, H., Keya, A.L., Berg, S., Nasralla, R., 2015. The effect of salinity, rock type and pH on the electrokinetics of carbonate-brine interface and surface complexation modeling. SPE Reservoir Characterisation and Simulation Conference and Exhibition. Presented at the SPE Reservoir Characterisation and Simulation Conference and Exhibition. Society of Petroleum Engineers, Abu Dhabi, UAE. <https://doi.org/10.2118/175568-MS>.
- Marzouk, I., 1999. Wettability and saturation in abu dhabi carbonate reservoirs. Middle East Oil Show and Conference. Presented at the Middle East Oil Show and Conference. Society of Petroleum Engineers, Bahrain. <https://doi.org/10.2118/53379-MS>.
- Minde, M.W., Zimmermann, U., Madland, M.V., Korsnes, R.I., Schulz, B., Gilbricht, S., 2020. Mineral replacement in long-term flooded porous carbonate rocks. *Geochim. Cosmochim. Acta* 268, 485–508. <https://doi.org/10.1016/j.gca.2019.09.017>.
- Morrow, N.R., 1990. Wettability and its effect on oil recovery. *J. Petrol. Technol.* 42, 1476–1484. <https://doi.org/10.2118/21621-PA>.
- Najafi-Marghmaleki, A., Barati-Harooni, A., Soleymanzadeh, A., Samadi, S.J., Roshani, B., Yari, A., 2016. Experimental investigation of effect of temperature and pressure on contact angle of four Iranian carbonate oil reservoirs. *J. Petrol. Sci. Eng.* 142, 77–84. <https://doi.org/10.1016/j.petrol.2016.02.004>.
- Okasha, T.M., Funk, J.J., Rashidi, H.N., 2007. Fifty years of wettability measurements in the arab-D carbonate reservoir. In: SPE Middle East Oil and Gas Show and Conference. Presented at the SPE Middle East Oil and Gas Show and Conference. Society of Petroleum Engineers, Manama, Bahrain. <https://doi.org/10.2118/105114-MS>.
- Prydatko, A.V., Belyaeva, L.A., Jiang, L., Lima, L.M.C., Schneider, G.F., 2018. Contact angle measurement of free-standing square-millimeter single-layer graphene. *Nat. Commun.* 9, 4185. <https://doi.org/10.1038/s41467-018-06608-0>.
- Rahimi, A., Honarvar, B., Safari, M., 2020. The role of salinity and aging time on carbonate reservoir in low salinity seawater and smart seawater flooding. *J. Petrol. Sci. Eng.* 187, 106739. <https://doi.org/10.1016/j.petrol.2019.106739>.
- Rocha, H.O., Costa, J.L.S., Carrasquilla, A.A.G., Carrasco, A.M.V., 2019. Petrophysical characterization using well log resistivity and rock grain specific surface area in a fractured carbonate pre-salt reservoir in the Santos Basin, Brazil. *J. Petrol. Sci. Eng.* 183, 106372. <https://doi.org/10.1016/j.petrol.2019.106372>.
- Rücker, M., Bartels, W.-B., Singh, K., Brussee, N., Coorn, A., Linde, H.A., Bonnin, A., Ott, H., Hassanizadeh, S.M., Blunt, M.J., Mahani, H., Georgiadis, A., Berg, S., 2019. The effect of mixed wettability on pore-scale flow regimes based on a flooding experiment in ketton limestone. *Geophys. Res. Lett.* 46, 3225–3234. <https://doi.org/10.1029/2018GL081784>.
- Ruidiaz, E.M., Winter, A., Trevisan, O.V., 2018. Oil recovery and wettability alteration in carbonates due to carbonate water injection. *J. Pet. Explor. Prod. Technol.* 8, 249–258. <https://doi.org/10.1007/s13202-017-0345-z>.
- Sharma, G., Mohanty, K., 2013. Wettability alteration in high-temperature and high-salinity carbonate reservoirs. *SPE J.* 18, 646–655. <https://doi.org/10.2118/147306-PA>.
- Shehata, A.M., Nasr-El-Din, H.A., 2015. Zeta potential measurements: impact of salinity on sandstone minerals. In: SPE International Symposium on Oilfield Chemistry. Presented at the SPE International Symposium on Oilfield Chemistry. Society of Petroleum Engineers, The Woodlands, Texas, USA. <https://doi.org/10.2118/173763-MS>.
- Sripal, E., James, L., 2018. Application of an optimization method for the restoration of core samples for SCAL experiments. *Petrophysics – SPWLA J. Form. Eval. Reserv. Descr.* 59, 72–81. [https://doi.org/10.30632/PETRO\\_059\\_1\\_A7](https://doi.org/10.30632/PETRO_059_1_A7).
- Teklu, T.W., Alameri, W., Kazemi, H., Graves, R.M., 2015. Contact angle measurements on conventional and unconventional reservoir cores. In: Proceedings of the 3rd Unconventional Resources Technology Conference. Presented at the Unconventional Resources Technology Conference. American Association of Petroleum Geologists, San Antonio, Texas, USA. <https://doi.org/10.15530/urtec-2015-2153996>.
- Wang, W., Gupta, A., 1995. Investigation of the Effect of Temperature and Pressure on Wettability Using Modified Pendant Drop Method. Presented at the SPE Annual Technical Conference and Exhibition. Society of Petroleum Engineers. <https://doi.org/10.2118/30544-MS>.
- Zhang, P., Austad, T., 2005. The relative effects of acid number and temperature on chalk wettability. In: SPE International Symposium on Oilfield Chemistry. Presented at the SPE International Symposium on Oilfield Chemistry. Society of Petroleum Engineers, The Woodlands, Texas. <https://doi.org/10.2118/92999-MS>.